JOURNAL OF SOLID STATE CHEMISTRY 114, 159–163 (1995)

Transport, Optical, and Magnetic Properties of the Conducting Halide Perovskite $CH_3NH_3SnI_3$

D. B. Mitzi, C. A. Feild, Z. Schlesinger, and R. B. Laibowitz

IBM T. J. Watson Research Center, P. O. Box 218, Yorktown Heights, New York 10598

Received February 28, 1994; accepted April 26, 1994

A low-temperature ($T \leq 100$°C) solution technique is described for the preparation of polycrystalline and single crystal samples of the conducting halide perovskite, $CH_3NH_3SnI_3$. Transport, Hall effect, magnetic, and optical properties are examined over the temperature range 1.8–300 K, confirming that this unusual conducting halide perovskite is a low carrier density p-type metal with a Hall hole density, $1/R_He \simeq 2 \times 10^{19}$ cm^{-3}. The resistivity of pressed pellet samples decreases with decreasing temperature with resistivity ratio $\rho(300\text{ K})/\rho(2\text{ K}) \simeq 3$ and room temperature resistivity $\rho(300\text{ K}) \simeq 7$ mΩ-cm. A free-carrier infrared reflectivity spectrum with a plasma edge observed at approximately 1600 cm^{-1} further attests to the metallic nature of this compound and suggests a small optical effective mass, $m^* \simeq 0.2$.

INTRODUCTION

The discovery of superconductivity in the cubic or distorted perovskites (1–4), $SrTiO_{3-\delta}$, $BaPb_{1-x}Bi(Sb)_xO_3$, and $Ba_{1-x}K_xBiO_3$, with transition temperatures between 0.25 and 30 K, as well as in the extensive family of layered perovskite cuprates with confirmed ambient pressure transitions up to 130 K (5), has spurred a significant interest in perovskite materials. Most recent interest has focused on the oxides since it is within this group that the majority of conducting perovskites are found. However, several insulating sulfide perovskites have also been reported (6–8) and there are many nonconducting halide perovskites, some of which are interesting magnetic systems (9). While most halide are good insulators, there exists an interesting class of conducting perovskite halides, $ASnX_3$, where A = Cs or CH_3NH_3 and X = Br or I (10–14).

The most common tin(II) coordination (15) consists of a trigonal–pyramidal arrangement of the three nearest neighbor tin–ligand bonds, with three other neighboring ligands at a considerably further distance, allowing room for the Sn(II) lone pair of electrons. Examples include $SnCl_2$, SnS, and $CsSnCl_3$(monoclinic form). Square pyramidal coordination is also common, occurring, for example, in SnO, $KSnF_3 \cdot \frac{1}{2} H_2O$, and α-$SnWO_3$. The perovskite tin halide compounds are unusual in that the tin(II) lone pair is stereochemically inactive, enabling tin(II) to achieve a regular octahedral coordination, presumably because electron density is transferred from the tin 5s nonbonding states into a conduction band (15).

Recently, the resistivity of several of these halide perovskites has been examined at temperatures above 77 K (12–14). $CsSnBr_3$ appears to be a small bandgap semiconductor ($E_g \approx 0.34$ eV) up to a temperature of 303 K, above which it displays a more metallic temperature-dependent resistivity (12, 14). $CsSnI_3$, in its metastable perovskite polytype, presents a metal-like temperature-dependent resistivity (13), with a room temperature resistivity of around 10 mΩ-cm. The resistivity data presented for $CH_3NH_3SnI_3$ by Yamada *et al.* (13) are less monotonic. At temperatures above 280 K, the resistivity drops significantly with decreasing temperature, with a room temperature resistivity around 20 mΩ-cm. Below 280 K, however, the resistivity looks flat or even increases slightly with decreasing temperature. In determining whether these materials are small band-gap semiconductors (16), semimetals (17), or metals, and given the superconducting properties of several related oxide perovskites, it is clearly interesting to investigate the low-temperature properties of these conducting halide perovskites and to address the nature of the carriers (electron vs hole, carrier concentration, effective mass, etc.). In this work, we concentrate on the cubic (at room temperature) perovskite $CH_3NH_3SnI_3$ and present resistivity, Hall effect, optical reflectivity, and magnetization data in the temperature range 1.8–300 K. The observation of a free-carrier infrared reflectivity spectrum with a plasma edge at approximately 1600 cm^{-1}, a positive temperature derivative of resistivity over the temperature range examined, and a measured Hall hole density of approximately 2×10^{19} cm^{-3} all confirm that this halide is a low carrier density metal with a small effective mass over the temperature range considered.

0022-4596/95 $6.00

EXPERIMENTAL

Polycrystalline $CH_3NH_3SnI_3$ can be prepared by precipitation from a hydriodic acid solution. Tin(II) iodide (10.40 g, 27.9 mmole) is first dissolved in 20 ml of a concentrated (57% by weight) aqueous HI solution in a test tube under flowing argon. An additional 8.0 ml of aqueous HI is added to a test tube containing $CH_3NH_2 \cdot HI$ (4.44 g, 27.9 mmole). Each solution is then gently heated to 90.0°C in a water/ethylene glycol bath to facilitate dissolution. After mixing the warm $CH_3NH_2 \cdot HI$ and SnI_2 solutions, the resulting yellow solution is cooled to room temperature by removing the tube from the hot bath. A black–green precipitate forms which can be filtered under flowing nitrogen and dried under flowing argon at 100°C for 5 hr. The yield is typically 67%. $CH_3NH_3SnI_3$ is air sensitive and decomposes in air within several hours. Consequently, all samples are stored and manipulated for the various measurements in an argon-filled glove box with oxygen and water levels below 1 ppm.

Room temperature X-ray powder diffraction shows the dried product to be free of starting materials and other pseudoternary phases. All reflections index on the basis of a cubic perovskite unit cell with lattice constant a = 6.2397(5) Å. Preliminary X-ray synchrotron and neutron diffraction studies demonstrate that the cubic room temperature structure does not survive to low temperatures. Analogous to $CH_3NH_3PbI_3$ (18), the structure distorts to lower symmetry through two transitions at approximately 275 and 100 K as the $CH_3NH_3^+$ cation orders at lower temperature. Details of these measurements will be presented elsewhere.

Small crystals, suitable for X-ray diffraction, can also be grown by the slow cooling of a concentrated HI solution under flowing argon. A 2.0-g charge of $CH_3NH_3SnI_3$ is prepared as above and equilibrated at 90.0°C in a water/ethylene glycol bath. Sufficient HI is added under flowing argon to dissolve the entire charge (about 11 ml). The solution is then cooled to −10.0°C at 2°C/hr. The small black crystals grow in a rhombic dodecahedral habit. Specimens were selected for X-ray analysis and mounted in a 0.3–mm glass capillary tube. Room temperature X-ray precession photography shows the crystals to be single with a cubic lattice constant a = 6.2 Å.

Electrical resistivity measurements were performed in a displex system using an airtight cell containing a four-point probe and a pressed pellet sample. The samples were pressed into 6-mm-diameter, 0.5- to 1.0-mm-thick circular pellets using approximately 45,000 psi applied pressure. Given the rather severe chemical reactivity of these materials, electrical contacts were made using spring-activated pins directly contacting the sample. Contact resistances of approximately 1 Ω could reproducibly be achieved and maintained down to low temperatures. At several temperatures during the temperature scan, an I–V scan was taken to confirm the ohmic nature of the contacts. Copper and carbon standards were also measured using the same sample geometry to calibrate the resistance probe and to ensure accurate resistivity values.

Resistivity and Hall measurements were also performed on similarly prepared pressed pellet samples using a van der Pauw geometry (19) with four spring-activated pins contacting the sample along the circumference of the circular sample. Measurements were made over the temperature range 2.0–300 K using fields up to 5 T and currents between 1 and 100 mA. The resistivity values obtained using the van der Pauw geometry are in very good agreement with those made using the four-point probe. Both n- and p-type silicon samples were examined in the same Hall geometry as the $CH_3NH_3SnI_3$ samples to verify the sign of the carriers.

To obtain the infrared reflectivity spectrum of $CH_3NH_3SnI_3$, roughly half of a polished pressed pellet sample was coated with gold and the reflectivity of the uncoated surface was measured relative to that of the gold-coated part. In this way, effects of roughness tend to cancel each other out and a reasonably accurate measure of the absolute reflectivity can be obtained using the known reflectivity of gold ($\gtrsim$99% for $\omega \lesssim$ 12,000 cm^{-1}). The sample was mounted on a kinematically stable movable arm with which either the gold-coated or uncoated parts of the sample could be readily moved in and out of the infrared beam. The infrared measurements were performed using a scanning interferometer with Hg-arc and Globar sources, and He-cooled bolometer detectors.

Magnetic measurements were performed in a Quantum Design SQUID magnetometer over the temperature range 1.8–300 K. Using a 10 Oe field, no evidence for superconductivity was found down to 1.8 K. In an effort to search for a Pauli susceptibility in these metallic materials, approximately 30- to 60-mg samples of $CH_3NH_3SnI_3$ and an applied field of 0.5 T were employed. The signal from the sample holder was measured separately and subtracted from the sample data.

RESULTS

Figure 1 shows the electrical resistivity, measured using the four-point technique, for $CH_3NH_3SnI_3$. The room temperature resistivity of the pressed pellet sample is $\rho(300\ K) \simeq 7$ mΩ-cm. The resistivity monotonically drops with decreasing temperature, with resistivity ratio $\rho(300\ K)/\rho(10\ K) \simeq 3$. Resistivity measurements down to 2 K, using the van der Pauw cell, verify that the resistivity saturates at low temperatures at slightly greater than 2 mΩ-cm and that the material does not superconduct at these temperatures. The exact form of the resistivity

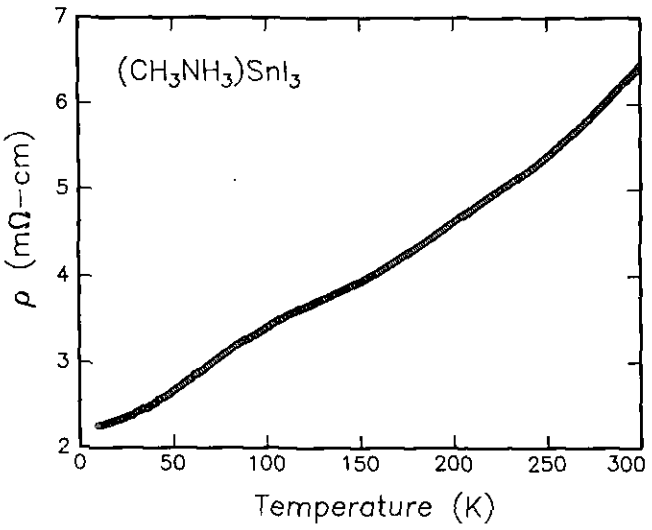

FIG. 1. Temperature dependence of the electrical resistivity of a pressed pellet $CH_3NH_3SnI_3$ sample measured using a four-point technique.

curve depends somewhat upon sample processing. Heating the sample above 200°C for prolonged periods, for example, can lead to some degradation, perhaps due to loss of iodine or methylamine from the material. This might account for the rising resistivity for temperatures below approximately 150 K in the data presented by Yamada *et al.* (13). The samples in this earlier study (13) were prepared by solid state reaction in an evacuated tube at 200°C, while the present samples were precipitated from solution and were always maintained at or below 100°C.

There is a small change in curvature of the resistivity, $\rho(T)$, at around 100 K. This reproducible but subtle feature in the resistivity data may be related to a structural distortion that occurs in this temperature range as the methylammonium cation orders in the structure. Several samples, measured after heating to approximately 195°C in Ar for several hours, displayed a more pronounced jump in resistivity at this temperature with a continuation of metallic behavior below the transition. At this point, it is uncertain whether the differences noted in these samples are the result of small numbers of defects introduced by higher temperature treatment or are perhaps the result of strain introduced by pressing the pellets that is relieved by heat treating the sample.

The carrier density, calculated from the Hall effect, and the Hall mobility at several different temperatures are shown in Fig. 2. The sign of the Hall voltage indicates that the carriers in $CH_3NH_3SnI_3$ are primarily holes. The Hall carrier density, calculated assuming a single band model, is roughly constant at temperatures above 100 K as is typical for simple metals. The average Hall constant is $R_H = 0.317$ cm^3/C, which corresponds to a Hall hole concentration, $n = 1/R_H e = 2.0(1) \times 10^{19}$ cm^{-3}. There is a slight increase in the Hall voltage (decrease in carrier concentration) below the structural transition at 100 K, with the Hall carrier concentration decreasing approximately 5% by 2 K. The small carrier concentration observed in this halide perovskite is roughly two orders of magnitude smaller than that in the copper or bismuth oxide based perovskite superconductors and corresponds to only 0.005 carriers per unit cell (or per tin atom). The Hall mobility is approximately 50 cm^2/V-sec at room temperature and rises to 140 cm^2/V-sec at low temperatures. In comparison, the room temperature Hall mobility in the superconducting (T_c = 81 K) cuprate, $Tl_2Ba_2CuO_{6+\delta}$, is approximately 1 cm^2/V-sec (20) and for

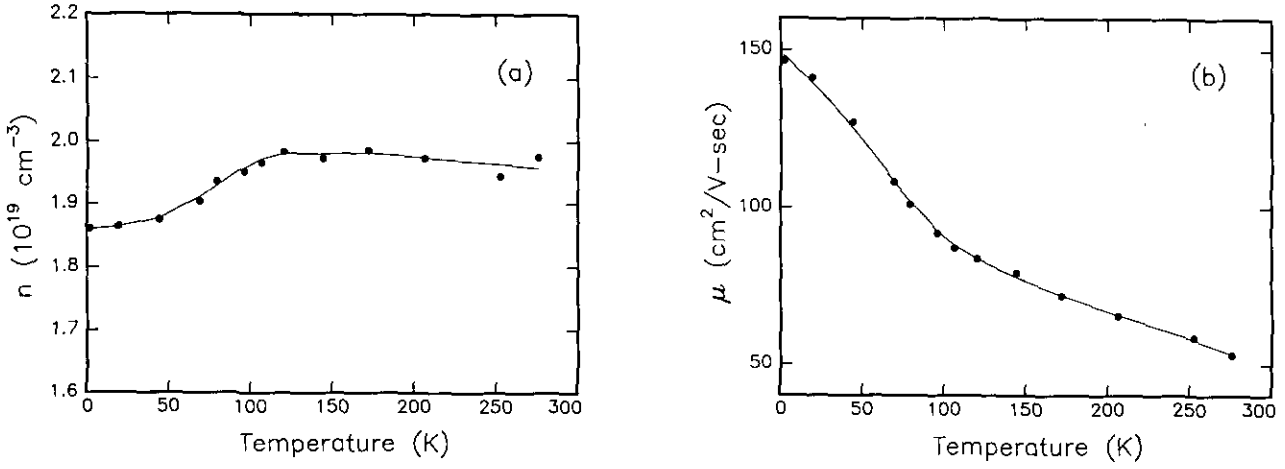

FIG. 2. (a) Hall hole concentration, $n = (R_H e)^{-1}$, and (b) Hall mobility, $\mu_H = R_H/\rho$, as a function of temperature for a pressed pellet sample of $CH_3NH_3SnI_3$. The solid lines are included as a visual guide.

$SrTiO_3$ is approximately 6 cm^2/V-sec for a wide range of doping levels (21).

Hall effect measurements were performed on several independent batches of $CH_3NH_3SnI_3$. While the Hall mobility of each of the samples examined closely matches the curve in Fig. 2, the Hall carrier concentrations show some variability between batches, ranging from 0.003–0.005 holes/tin atom. Samples within a given batch consistently yield the same concentration. Given the very small carrier concentrations present in these materials, small numbers of cation or anion defects could easily account for this variability. For example, the removal of only 0.002 $CH_3NH_3^+$/unit cell should provide the full range of observed carrier concentrations. Both cation and anion vacancies are often known to exist in perovskite and perovskite-related materials (22, 23).

An infrared reflectivity spectrum is shown for $T \simeq 30$ and 280 K in Fig. 3. This reflectivity is characteristic of a conductor in that it approaches unity as the frequency approaches zero, and of a metal in that it increases with decreasing temperature at low frequency. The rapid decrease in R above 1000 cm^{-1} and the reflectivity minimum near 1600 cm^{-1} result from the real part of the dielectric coefficient crossing zero, i.e., the plasma edge. From these data one can infer the ratio of carrier density to carrier mass, n/m^*, where m^* is the ratio of the optical mass to the mass of a free electron. The optical mass relevant here is evaluated at about the frequency of the plasma edge, and will tend to be smaller than the low frequency or specific heat mass, since enhancements due to inelastic scattering at lower energies are not operative at this frequency. Within an accuracy of about ±15% these data imply a carrier density to mass ratio of

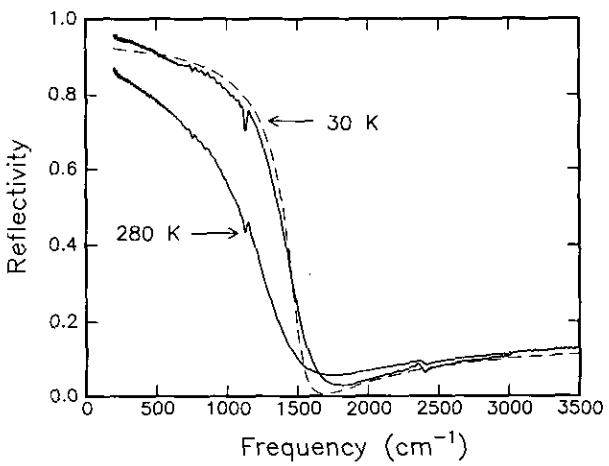

FIG. 3. Infrared reflectivity spectrum on a pressed pellet sample of $CH_3NH_3SnI_3$ at $T = 30$ and 280 K. The dashed line shows a fit to a Drude formula for the low-temperature data using $n/m^* = 1.25 \times 10^{20}$ cm^{-3}, a high-frequency dielectric constant of 5, and a scattering rate of roughly 140 cm^{-1}.

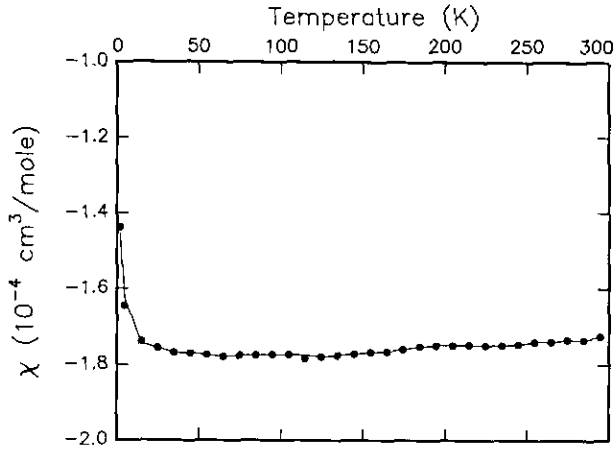

FIG. 4. Magnetic susceptibility as a function of temperature for $CH_3NH_3SnI_3$ in an applied field of 0.5 T. The solid line is included as a visual guide.

$n/m^* \simeq 1.25 \times 10^{20}$ cm^{-3}. This value is an order of magnitude lower than in superconducting cuprate or bismuthate compounds, and two orders of magnitude lower than in conventional metals. Combining this ratio with the value of the carrier concentration derived from the Hall effect (measured on a sample from the same batch) leads to an optical mass $m^* = 0.16(5)$. This small effective mass is consistent with the fairly high Hall mobilities and is more analogous to the small effective masses observed (24, 25) in $BaPb_{1-x}Bi_xO_3$ ($m^* \simeq 0.3$–0.8) than to the enhanced masses observed in the cuprate perovskites or in $SrTiO_3$. This suggests that the Fermi level, E_f, resides in a rather broad s-like band as in the $BaPb_{1-x}Bi_xO_3$ system, where E_f falls within a band of primarily O $2p$ and Pb–Bi $6s$ character.

The infrared reflectivity in the frequency range $\omega \lesssim 2000$ cm^{-1} can be crudely fit using a Drude formula with the above-mentioned n/m^* ratio, a high frequency dielectric constant of 5, and a scattering rate of roughly 140 cm^{-1} at 30 K. There are, however, significant deviations from a simple Drude form, presumably due to a frequency dependence of the scattering rate, associated with the same inelastic scattering processes that are responsible for the temperature dependence of the dc resistivity.

The magnetic susceptibility for $CH_3NH_3SnI_3$ is shown in Fig. 4. In principle, the observed magnetic susceptibility for this compound should be a sum of the contributions from core diamagnetism, Pauli paramagnetism, and Landau diamagnetism. To get an independent measure of the core diamagnetism, the insulating compounds SnI_2 and $CH_3NH_2 \cdot HI$ were measured. The sum of the susceptibilities of these two insulating compounds should equal the core diamagnetism in metallic $CH_3NH_3SnI_3$

and, in fact, this value agrees fairly well with the value calculated using tabulated (26) atomic core susceptibility data ($-1.8(1) \times 10^{-4}$ cm^3/mole vs -1.9×10^{-4} cm^3/mole, respectively). Comparison with the measured susceptibility of $CH_3NH_3SnI_3$, $\chi = -1.8(1) \times 10^{-4}$ cm^3/mole, indicates that to within the accuracy of the measurement, the measured susceptibility can be completely accounted for by core susceptibility. These measurements are consistent with the small mass and carrier concentrations implied by the Hall and infrared data. Using $m^* = 0.16$, $n = 2.0 \times 10^{19}$ cm^{-3} and a free carrier model in which $\chi_p \propto m^* n^{1/3}$, we expect a Pauli susceptibility on the order of 1×10^{-6} cm^3/mole, which is below our ability to resolve. Additionally, given the small effective mass, Landau diamagnetism may become a more significant factor and may hinder attempts to distinguish a Pauli susceptibility in these materials using magnetic measurements.

CONCLUSIONS

The perovskite $CH_3NH_3SnI_3$ has been shown to be a low carrier density metal in the temperature range 1.8–300 K with no transition to the superconducting state in this temperature range. The room temperature resistivity on pressed pellet samples is approximately 7 mΩ-cm for samples prepared by a low-temperature precipitation technique. The resistivity drops with decreasing temperature with a resistivity ratio $R(300\text{ K})/R(2.0\text{ K}) \simeq 3$. A plasma edge is also observed in the infrared reflectivity spectrum at 1600 cm^{-1}, corresponding to a carrier concentration to mass ratio of $n/m^* \simeq 1.25 \times 10^{20}$ cm^{-3}. Combining this ratio with a Hall carrier concentration of approximately 2×10^{19} holes/cm^3 implies a rather light optical mass of $m^* \simeq 0.2$. The apparent broad band conduction in this material is reminiscent of that observed in $BaPbO_3$ with, however, a carrier concentration lower by a factor of 10.

There are several examples of oxide perovskites that when properly doped yield superconducting materials. Doped $SrTiO_3$, with an electron density in the range 10^{18}–10^{20} cm^{-3}, is superconducting at approximately 0.25 K (1). The cuprate high-temperature superconductors have a hole concentration of approximately 10^{21} cm^{-3}, while the $(Ba,K)(Bi,Pb)O_3$ superconductors, with transitions as high as 30 K, also have electron densities of the order 10^{21} cm^{-3} for compositions in the superconducting regime. In all the cases above, the ability to dope or tune the carrier concentration has played a key role in observing superconductivity. Given the low carrier density in $CH_3NH_3SnI_3$ in its as-prepared state, it will be interesting to see whether it is possible to dope this halide perovskite and to study what effect this has on its physical properties.

ACKNOWLEDGMENTS

The authors thank B. Scott, D. Beach, and E. Suard for stimulating discussions, M. Ritter for use of a displex system to measure resistivity on the air-sensitive samples, and J. Lacey for technical help during the Hall measurements.

REFERENCES

1. J. F. Schooley, W. R. Hosler, and M. L. Cohen, *Phys. Rev. Lett.* **12,** 474 (1964).
2. A. W. Sleight, J. L. Gillson, and P. E. Bierstedt, *Solid State Commun.* **17,** 27 (1975).
3. R. J. Cava, B. Batlogg, G. P. Espinosa, A. P. Ramirez, J. J. Krajewski, W. F. Peck, Jr., L. W. Rupp, Jr., and A. S. Cooper, *Nature* **339,** 291 (1989).
4. L. F. Mattheiss *et al.*, *Phys. Rev. B* **37,** 3745 (1988); R. J. Cava *et al.*, *Nature* **332,** 814 (1988).
5. A. Schilling, M. Cantoni, J. D. Guo, and H. R. Ott, *Nature* **363,** 56 (1993).
6. Von H. Hahn and U. Mutschke, *Z. Anorg. Allg. Chem.* **288,** 269 (1956).
7. M. Saeki, Y. Yajima, and M. Onoda, *J. Solid State Chem.* **92,** 286 (1991).
8. B.-H. Chen, W. Wong-Ng, and B. W. Eichhorn, *J. Solid State Chem.* **103,** 75 (1993).
9. L. J. de Jongh and A. R. Miedema, *Adv. Phys.* **23,** 1 (1974).
10. D. E. Scaife, P. F. Weller, and W. G. Fisher, *J. Solid State Chem.* **9,** 308 (1974).
11. D. Weber, *Z. Naturforsch. B* **33,** 862 (1978).
12. S. J. Clark, C. D. Flint, and J. D. Donaldson, *J. Phys. Chem. Solids* **42,** 133 (1981).
13. K. Yamada, T. Matsui, T. Tsuritani, T. Okuda, and S. Ichiba, *Z. Naturforsch. A* **45,** 307 (1990).
14. R. L. Narayan and S. V. Suryanarayana, *Mater. Lett.* **11,** 305 (1991).
15. J. D. Donaldson and S. M. Grimes, *Rev. Silicon, Germanium, Tin, Lead Compd.* **8,** 1 (1984).
16. I. Lefebvre, P. E. Lippens, M. Lannoo, and G. Allan, *Phys. Rev. B* **42,** 9174 (1990).
17. D. E. Parry, M. J. Tricker, and J. D. Donaldson, *J. Solid State Chem.* **28,** 401 (1979).
18. Q. Xu, T. Eguchi, H. Nakayama, N. Nakamura, and M. Kishita, *Z. Naturforsch. A* **46,** 240 (1990).
19. L. J. van der Pauw, *Philips Res. Rep.* **13,** 1 (1958).
20. Y. Kubo and T. Manako, *Physica C* **197,** 378 (1992).
21. H. P. R. Frederikse, W. R. Thurber, and W. R. Hosler, *Phys. Rev.* **134,** A442 (1964).
22. C. Michel and B. Raveau, *Rev. Chim. Miner.* **21,** 407 (1984).
23. F. Galasso, "Structure, Properties and Preparation of Perovskite-Type Compounds," pp. 10–11. Pergamon Press, New York, 1969.
24. K. Kitazawa, A. Katsui, A. Toriumi, and S. Tanaka, *Solid State Commun.* **52,** 459 (1984).
25. S. Tajima, K. Kitazawa, and S. Tanada, *Solid State Commun.* **47,** 659 (1983).
26. K.-H. Hellwege and A. M. Hellwege (Eds.) "Landolt-Börnstein" (new series), Vol. II/16, pp. 3,402. Springer–Verlag, Heidelberg, 1986.